Outdoor-to-Indoor Coverage in High Frequency Bands

Eliane Semaan, Fredrik Harrysson, Anders Furuskär, Henrik Asplund
Ericsson Research, Ericsson AB, Sweden,
Email: {eliane.semaan, fredrik.harrysson, anders.furuskar, henrik.asplund}@ericsson.com

***Abstract*—With the continuous growth in connected devices and the need for larger bandwidth channels and greater data speeds, operating at high frequencies can be advantageous for future mobile communications in general, and for 5G-networks in particular. In this paper, the indoor coverage at different high frequencies, namely 10, 30 and 60 GHz has been analyzed in the context of a single building scenario with an outdoor deployed base station and low load conditions. These specific frequencies are only meant as examples to illustrate the general trends of how coverage varies across the frequency range. A main observation, also subject to the assumptions made on propagation, antenna pattern and bandwidth size, is that outdoor to indoor coverage with down link (DL) user throughput higher than 10 Mbps, and in certain cases higher than 100 Mbps, is possible at 10 GHz and above. The case with carrier frequencies up to 30 GHz is more challenging however still manageable, whereas providing outdoor to indoor coverage at 60 GHz may be quite difficult for some building types. It has also been seen that the use of high gain antennas is crucial at high frequencies and that the deployment density depends on the type of building, in other words, on the exterior wall material, interior layout, wall material and building size.**

I. Introduction

The main reason for looking into higher frequencies is to find new spectrum to use, which will hopefully manifest in much wider bands than what is currently used for mobile systems.

However, there are reasons to be skeptical about the use of higher frequency bands in some deployments due to the challenging path loss characteristics as these waves are subject to several loss factors, starting from the high atmospheric attenuation, rain fade, foliage attenuation, building and wall penetration, diffraction and body/obstruction loss.

While some of the mentioned loss aspects may be considered as minor problems for lower frequency bands, their impact may become severe in high frequency ranges. This increased path loss limits potential communications range, however high frequency waves allow for smaller frequency reuse distances, larger bandwidth and small beam width allowing for higher gain values, which in turn can compensate to some extent for the experienced higher path-loss.

During the last decades a number of studies on building penetration loss (BPL) at mainly lower cellular frequency bands but also in millimeter-wave bands has been described in literature [1–9]. However, there is still an urgent need for valid outdoor-to-indoor models that cover the entire spectrum from common cellular up to millimeter-wave frequencies.

This paper presents new simple candidate models and evaluation results of the performance of outdoor deployed small cells targeting single building indoor coverage at frequencies above 6 GHz. Results are presented in terms of propagation gain maps as well as user throughput for the different example frequencies. The outline of the paper is as follows: Section II introduces the propagation model used, Section III gives a description of the single building scenario and the simulation assumptions, Section IV presents the simulation results and finally conclusions are given in Section V.

II. Frequency-dependent propagation models

The propagation model is composed of several sub-models taking into account free space propagation in line-of-sight, diffraction modeling in none-line-of-sight, BPL, and indoor loss. The basis for each of these sub-models has been taken by selecting appropriate models described in the COST 231 Final Report [10]. These include the Ericsson micro-cell model for outdoor propagation [10, Section 4.5.2], the general building penetration model [10, Section 4.6], and the linear attenuation model for indoor propagation [10, Section 4.7.2]. The models have been further updated to include relevant frequency-dependency as presented in this section, mainly based on measurements and estimations performed by different sources. It should be noted that these new models have been developed to create an approximate qualitative match with the diverse and limited measurements that are available.

Determination of the propagation path loss from an outdoor node (base station) to an indoor node (terminal) consists of evaluating four candidate paths, one through each external wall, and selecting the path resulting in the lowest total path loss when adding up the outdoor loss, the BPL, and the indoor loss. In many cases this will be the path through the wall facing the base station but for terminals on the far side of the building a propagation path that diffracts around a building corner and enters through a side wall may result in a lower total path loss, particularly if the indoor loss is high, see Fig. 1.

A. Building penetration loss

In high frequency bands, the material characteristics of the building have a major impact on defining the penetration loss pattern, thus the BPL can be significantly different for different buildings. The BPL is calculated based on the mean transmitted power through different building materials.

In our simulations we refer to two different building wall configuration examples, namely ”old house” and ”new house”. The ”old house” assumption corresponds to a composite model

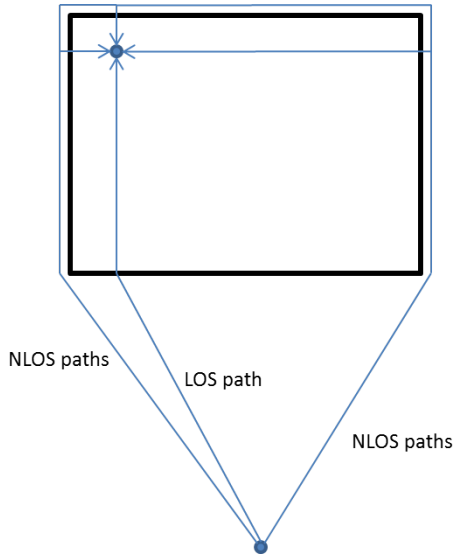

Fig. 1. Illustration of propagation paths.

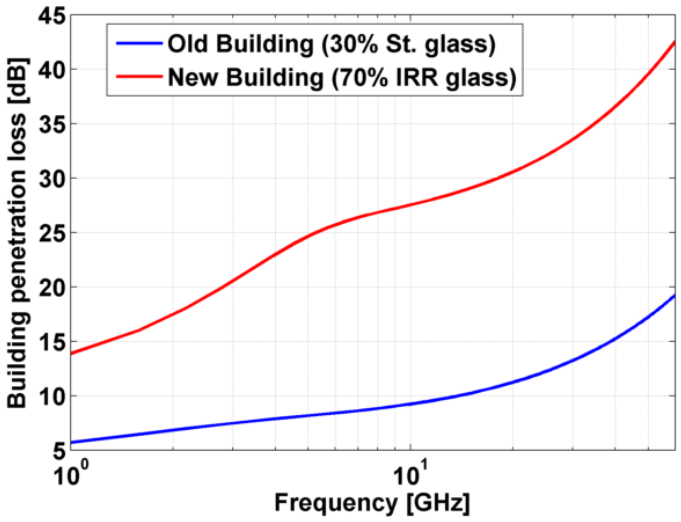

Fig. 2. Building penetration loss – combined models.

with 30% "standard" glass windows and 70% concrete wall. Whereas, the "new house" composite model corresponds to 70% Infrared Reflective Glass (IRR) glass windows, common in modern energy saving houses, and 30% concrete wall. To model the frequency dependency penetration loss (including reflection loss) for single materials a simple model structure has been used to approximately match the results that is found in [9, 11–14].

The transmission loss of a single standard window glass is here modeled as

$$L_{glass,dB} = 0.1 f_{GHz} + 1, \tag{1}$$

and for the concrete wall as

$$L_{conc,dB} = 4 f_{GHz} + 5, \tag{2}$$

where $L_{glass,dB}$ is the effective glass transmission loss in dB and f_{GHz} is the frequency expressed in GHz. The total transmission loss through a "standard" window is then modeled by $2L_{glass,dB}$, and by $3L_{glass,dB} + 20$, for standard two-glass windows, and the more modern three-glass IRR windows, respectively. Here the loss of the IRR layer was set to 20 dB which represent an effective additional loss of the window due to the IRR layer (the transmission loss of such glass, specifically, may be well above 30 dB). The models are illustrated in Fig. 2.

In addition to the loss illustrated above, the angular wall loss model from [10, Section 4.6.2] is used in the simulator to count for the additional loss that can be experienced depending on the incident angle. This is modeled as

$$L_{ang,dB} = 20(1 - \cos\theta)^2, \tag{3}$$

where θ is the angle of incidence. For NLOS propagation this angle is set to $\pi/3$, i.e. the angle of incidence corresponding to an average angular loss. The maximum angular loss is here maximized to 20 dB.

B. Indoor wall loss

The indoor environment is assumed to be open, with standard glass, alternatively plaster, indoor walls. Hence, the loss model per wall is calculated as a function of the carrier frequency and with an average wall distance of 4 m. Two different indoor loss models are considered; model 1, and model 2. Model 1 assumes a wall loss equal to that of a single standard glass layer and follows (1), as

$$L^{(1)}_{iwall,dB} = L_{glass,dB}, \tag{4}$$

Whereas indoor loss model 2 is mainly based on measurements performed in [9]. The indoor wall loss in the latter case is estimated as

$$L^{(2)}_{iwall,dB} = 0.2 f_{GHz} + 1.7, \tag{5}$$

Indoor wall loss model 1 may tend to underestimate the indoor loss at high frequencies. For instance, it can be observed from the measurements performed in [9] that after passing the first distance reaching interior walls inside the building, the signal tends to find a relatively better path to the receiver (e.g. through open doors, corridors, etc.) than in the case of a receiver standing right behind the exterior wall (or within the first few meters).

On the other hand, model 2 may tend to overestimate the dB/m indoor loss as we interpolate it to provide an estimated loss deep inside a large building, especially as the measurements in [9] provide an indication of the indoor loss for up to 10 m. As it will be shown in Section IV, the assumptions on the indoor loss model will have a significant impact on the results. Thus, both models are considered in this study, which in turn provides an insight into the sensitivity of the results towards the assumptions made on indoor loss models.

It should be noted that inner walls may be the glass/plasterboard ones as we consider, but also the thick concrete load-bearing ones which have a loss in the order of an outer wall. The latter case would result in a totally different indoor loss pattern. In addition, other obstructions such as

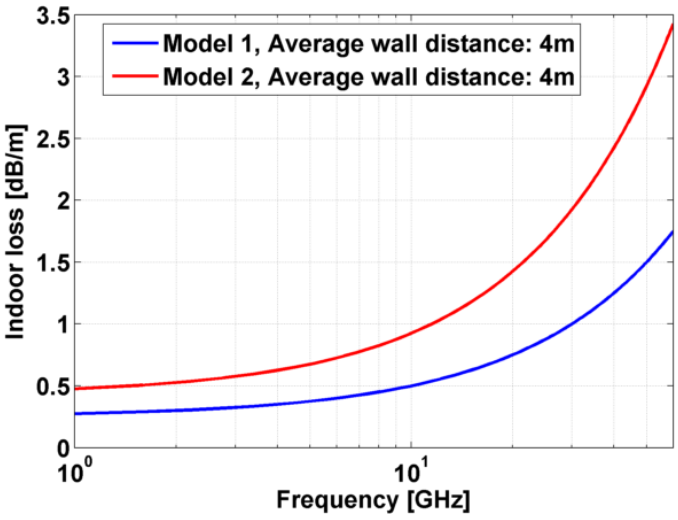

Fig. 3. Indoor loss models for different frequencies.

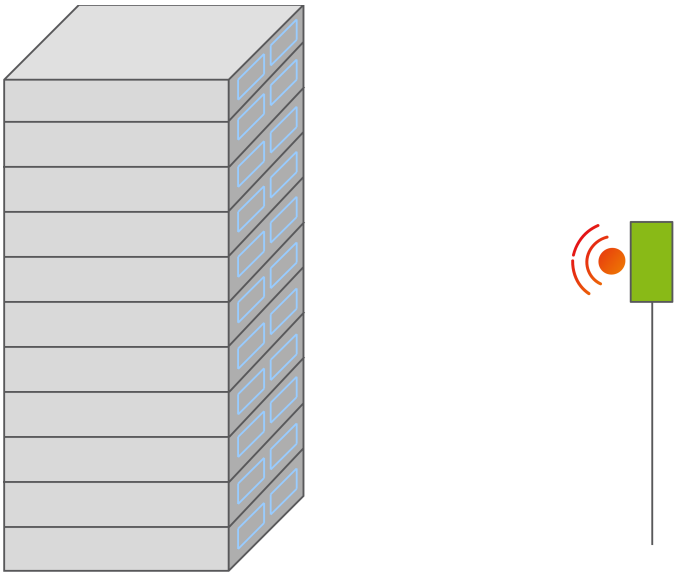

Fig. 4. Single building deployment (not to scale).

metal white boards could be mounted on the walls causing a higher loss.

C. Body loss

The body loss, mainly caused by the user being in a position that blocks the strongest signal from a transmitter may be severe in some cases. For instance, at high frequencies, it may happen that the mobile terminal or user equipment (UE) gets completely blocked by the user (i.e. absence of strong multipath signals), which may result in high loss values, which in turn leads to a high variance (shadow fading) in received signal [15, 16]. Hence, we assume in this study that there are always some reflections in the room.

The second factor that adds to the total body loss is the loss arising due to the UE antenna being blocked by the hand. This loss highly depends on the way the user is holding the UE as well as on the antenna placement. Existing measurements have shown values between 3 and 15 dB for different holding positions and antenna placements [16]. In this study, we assume that the UE is used in browse mode (e.g. high data rate use case) and that the antenna placement is clever, possibly more than one antenna element is available such that at least one antenna element is not affected much by the hand (selection diversity).

As a result, the average body loss, considering randomly oriented users, was here modeled according to $L_{body,dB} = f_{GHz}/60 + 3$, assuming a loss of 3 dB due to the hand/finger. Thus, the frequency dependency of the average body (shadowing) loss will have negligible impact on these simulations.

III. Single Building Scenario

A single building deployment is considered in order to give an indication on the deployment density that is needed to be able to provide indoor coverage in the entire building given a minimum achievable user throughput threshold. As depicted in Fig. 4, an outdoor deployed base station is placed at a certain height and distance from the targeted building, which may correspond to the case where a base station is mounted on the exterior wall of another building. The main deployment and simulation parameters are available in Table I.

TABLE I. Deployment and Simulation Parameters

Deployment/simulation parameters	Parameter value
Number of buildings	1
Building size [m]	40x40x63
Number of floors	21
Number of base stations	1
Distance between BS and building [m]	35
BS height [m]	31.5
BS output power [dBm]	33
Bandwidth [MHz]	100
BS antenna	Wall-mounted HV antenna
BS antenna gain [dBi]	(8, 16.3)
UE location	Indoor
UE antenna	Isotropic
Carrier frequencies [GHz]	10, 30, 60
Average packet size [Mbyte]	1
Average Poisson arrival intensity [Packets/100 s]	8

IV. Simulation Results

Results based on simulations performed in a static LTE system level simulator, implementing the afore-mentioned propagation models, are presented in terms of propagation gain maps (Section IV-A) and throughput (Section IV-B).

A. Propagation gain maps

In order to show the impact of the two different indoor loss models on the indoor coverage, 3D indoor gain maps are presented for the two studied building types. A base station gain of 8 dBi is assumed in this case. Fig. 5 to Fig. 7 illustrates the gain map in the target building at 10, 30 and 60 GHz respectively. It can be noticed that the different indoor models

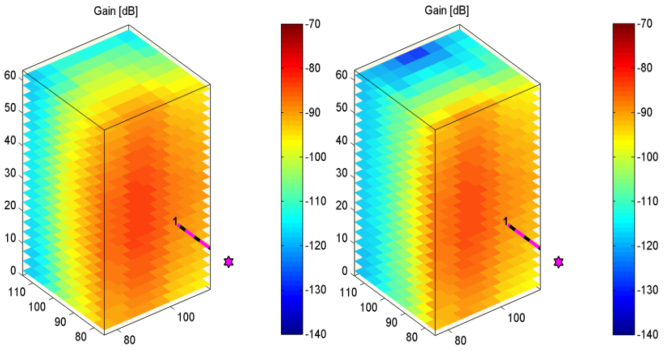

Fig. 5. Gain map for old building type at 10 GHz with indoor model 1 (left) and model 2 (right).

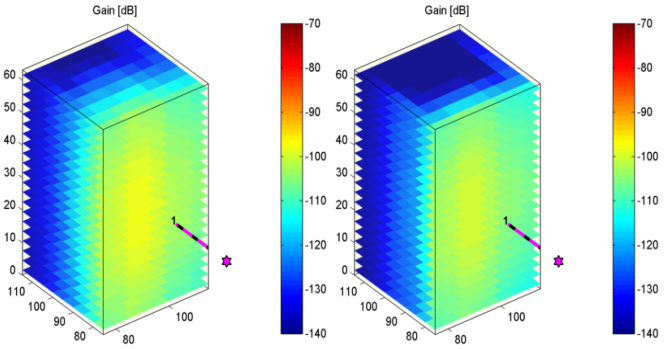

Fig. 6. Gain map for old building type at 30 GHz with indoor model 1 (left) and model 2 (right).

have a significant impact on the coverage especially as the user moves deep inside the building.

In general, gain levels allowing for data rates in the order of 100 Mbps (i.e. -118 dB total gain) can be observed at 10 GHz while more challenging levels, yet still allowing for a data rate of 10 Mbps (i.e. -129.4 dB total gain) in large parts of the building, can be seen in case of frequencies around 30 GHz. On the other hand, the indoor coverage tends to get extremely poor at 60 GHz with a total gain below -130 dB in the majority of the building making providing the required coverage exceedingly difficult even with a denser outdoor deployment as the high indoor loss would remain a challenging factor.

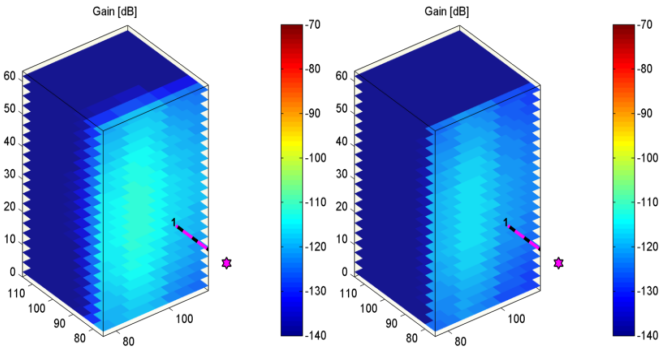

Fig. 7. Gain map for old building type at 60 GHz with indoor model 1 (left) and model 2 (right).

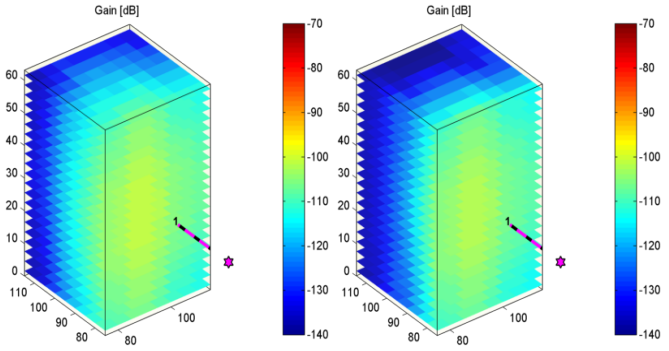

Fig. 8. Gain map for new building type at 10 GHz with indoor model 1 (left) and model 2 (right).

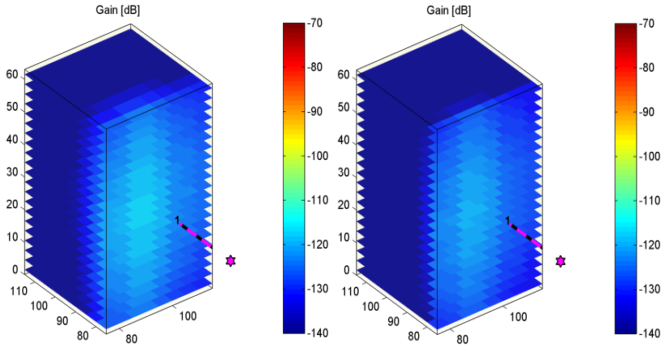

Fig. 9. Gain map for new building type at 30 GHz with indoor model 1 (left) and model 2 (right).

Gain maps for the new building type are presented in Fig. 8 to Fig. 10. It can be seen that outdoor-to-indoor coverage in the entire building can still be conceivable at 10 GHz assuming a slightly denser deployment. If compared to the old building type, the propagation conditions in this case become quite challenging already at 30 GHz as the propagation gain map is to some extent comparable to that in the former case, however at 60 GHz. As a result, outdoor deployments targeting indoor users become in this case a questionable solution at 30 GHz and above due to the observed extreme coverage degradation.

B. *User throughput*

Providing a capacity of 10 Mbps and 100 Mbps in the entire building assuming a bandwidth of 100 MHz, would

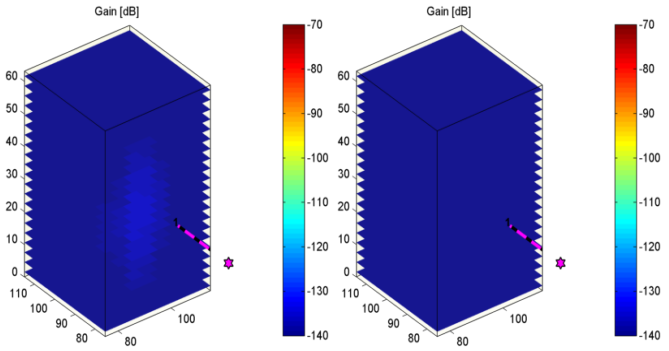

Fig. 10. Gain map for new building type at 60 GHz with indoor model 1 (left) and model 2 (right).

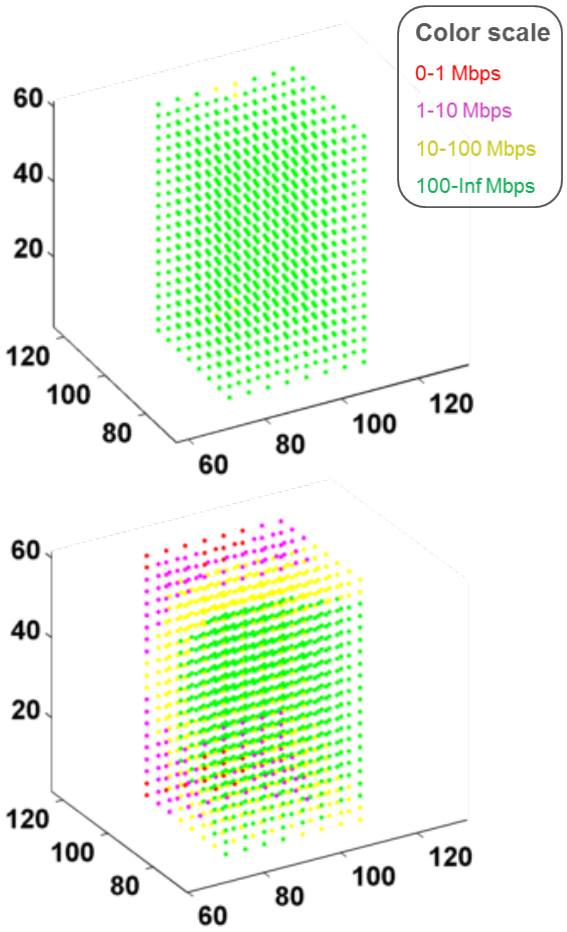

Fig. 11. DL user throughput map at 10 GHz for old building type (left) and new building type (right).

require at least -11.4 dB and 0 dB signal to noise ratio (SNR), respectively, according to Shannon-Hartley theorem:

$$C = B\log_2(1 + S/N), \tag{6}$$

where C is the channel capacity (bps), B is the bandwidth of the channel (Hz), and S/N is the SNR. Given an output power of 33 dBm and assuming a noise figure (NF) in the order of 9 dB, the minimum required total gain G_{min} can be calculated as

$$G_{min,dB} = -P_{Tx,dBm} + SNR_{dB} + kTB_{dBm} + NF_{dB} \tag{7}$$

Thus, the resulting total gain for a capacity of 10 Mbps and 100 Mbps in the entire building become -129.4 dB and -118 dB, respectively.

As shown in Section IV-A, a higher base station antenna gain is needed for some frequency ranges and building types. Hence, in this section, performance results are presented in terms of DL user throughput assuming a base station antenna gain of 16.3 dBi. As we are primarily interested in coverage, the focus has been on simulating low-load cases.

The DL user throughput map at 10 GHz is shown in Fig. 11 for the old and new building models, using indoor model 1 and assuming an output power of 33 dBm and a 100 MHz bandwidth. The higher BPL in the new building type

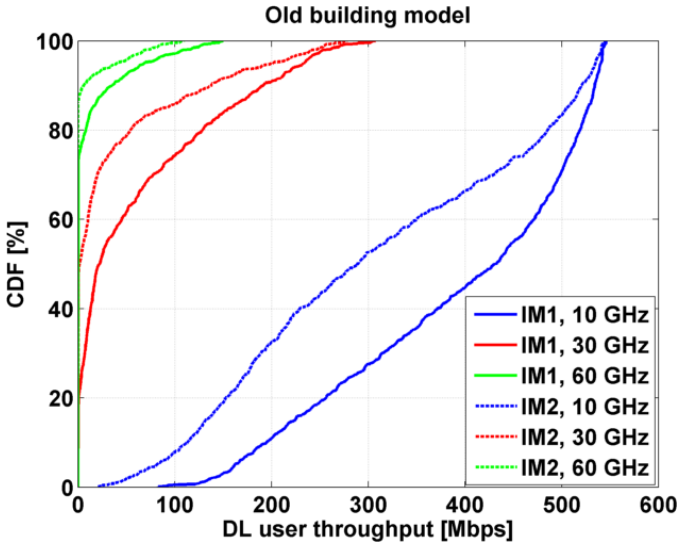

Fig. 12. Old building type - cumulative distribution of the DL user throughput.

translates here into lower user throughput and worse coverage. The complete set of results for 10, 30 and 60 GHz, different building types and indoor models are presented in a more concise manner as cumulative distributions.

Fig. 12 shows the cumulative distribution of the DL user throughput that can be expected in an old building at three different frequency ranges and assuming two different indoor models, i.e. IM1 and IM2. Even though indoor model 2 makes reaching high data rates more challenging, a user throughput above 100 Mbps can still be reached for approximately 92% of the users at 10 GHz. At 30 GHz, 65% and 41% of the users have a DL user throughput higher than 10 Mbps, respectively for indoor model 1 and indoor model 2 assumptions. Thus, more than one base station would be needed in this case to provide coverage in the entire building with a at least 10 Mbps DL user throughput. At 60 GHz, providing at least 10 Mbps throughput in the entire building would require a quite dense base station deployment; as shown in Fig. 12, only 19%, respectively 9% of all users (basically the ones located within a very short distance from the outer wall) could reach a DL throughput of 10 Mbps using indoor model 1 and 2.

Fig. 13 shows the cumulative distribution of the DL user throughput in the new building model. As it was the case with the old building model, reaching at least 100 Mbps at 10 GHz is possible, however in this case a denser base station deployment is needed as only 53% and 32% of the users, respectively for IM1 and IM2, can reach up to 100 Mbps with the current setup. Frequencies in the 30 GHz range are more challenging for this type of buildings as the coverage here is comparable to that of the old building model at 60 GHz (i.e. 17% and 9% of the users reaching at least 10 Mbps DL throughput). For frequencies in the 60 GHz range and above, providing outdoor to indoor coverage may be extremely difficult, given that not even users with the most favorable locations could be served. Hence, a denser outdoor deployment and higher antenna gains may not be a solution in this case. It should be noted that EIRP considerations may place a limit on the antenna gain.

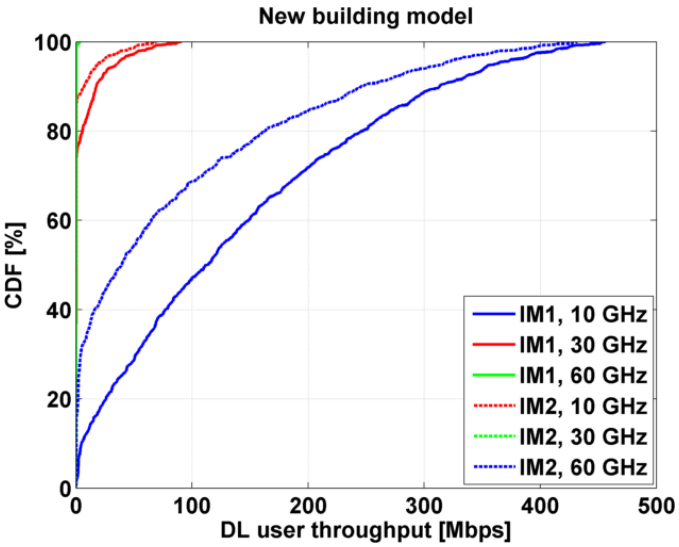

Fig. 13. New building type - cumulative distribution of the DL user throughput.

V. Conclusions

The indoor DL coverage at a range of frequencies above 6 GHz (up to 60 GHz) has been analyzed in the context of a single-building scenario with an outdoor deployed base station and low load conditions. The specific frequencies used in the simulations (10, 30, and 60 GHz) are arbitrarily selected and intended as examples to illustrate the general trends of how coverage varies across the frequency range.

In general, outdoor-to-indoor coverage with DL user throughput higher than 100 Mbps can be achievable at 10 GHz with a low deployment density. The case with carrier frequencies in the range of 30 GHz may be considered as more challenging, especially for the new building model. However, providing DL user throughput of at least 10 Mbps in the entire building is still conceivable in old building models with a relatively low base station density. On the other hand, outdoor-to-indoor coverage at 30 GHz in new building models and at 60 GHz in old building models have shown similar patterns, thus a larger number of base stations is required to meet the throughput threshold. A less promising scenario is seen at 60 GHz and above in the new building model where outdoor-to-indoor coverage may be extremely difficult. In addition, the significance of using high gain antennas at high frequencies (i.e. 30 GHz and above) has been highlighted. Moreover, it has been shown that factors such as building type, exterior wall material, interior layout, etc., are of crucial importance at high frequencies.

Further studies should cover scenarios with multiple buildings, or complete cities, enabling modeling the effects of diffractions and reflections.

References

[1] L. H. Loew, Y. Lo, M. Laflin, and E. E. Pol, "Building penetration measurements from low-height base stations at 912, 1920, and 5990 MHz," NTIA, Boulder, CO, Tech. Rep. NTIA Technical Report TR-95-325, Oct. 1995.

[2] A. F. Elrefaie and M. Shakouri, "Propagation measurements at 28 GHz for coverage evaluation of local multipoint distribution service," in *Proceedings Wireless Communications Conference*, 1997, pp. 12–17.

[3] P. F. M. Smulders and L. M. Correia, "Characterisation of propagation in 60 GHz radio channels," *Electronics Communication Engineering Journal*, vol. 9, no. 2, pp. 73 –80, Apr. 1997.

[4] G. Durgin, T. S. Rappaport, and H. Xu, "5.85-GHz radio path loss and penetration loss measurements in and around homes and trees," *Communications Letters, IEEE*, vol. 2, no. 3, pp. 70–72, 1998.

[5] J. Medbo, F. Harrysson, H. Asplund, and J. E. Berg, "Measurements and analysis of a MIMO macrocell outdoor-indoor scenario at 1947 MHz," in *Proc. IEEE VTC 2004-Spring*, vol. 1, Milan, Italy, May 2004, pp. 261–265.

[6] J. Medbo, J. Furuskog, M. Riback, and J.-E. Berg, "Multi-frequency path loss in an outdoor to indoor macrocellular scenario," in *3rd European Conference on Antennas and Propagation (EuCAP)*, March 2009, pp. 3601–3605.

[7] H. Zhao, R. Mayzus, S. Sun, M. Samimi, J. Schulz, Y. Azar, K. Wang, G. Wong, F. Gutierrez, and T. Rappaport, "28 GHz millimeter wave cellular communication measurements for reflection and penetration loss in and around buildings in New York City," in *Communications (ICC), 2013 IEEE International Conference on*, June 2013, pp. 5163–5167.

[8] J. Lu, D. Steinbach, P. Cabrol, P. Pietraski, and R. V. Pragada, "Propagation characterization of an office building in the 60 GHz band," in *European Conf. on Ant. and Prop. (EuCAP)*, The Hague, The Netherlands, April 2014, pp. 922 – 926.

[9] C. Larsson, F. Harrysson, B.-E. Olsson, and J.-E. Berg, "An outdoor-to-indoor propagation scenario at 28 GHz," in *Antennas and Propagation (EuCAP), Proceedings of the 6th European Conference on*, The Hague, The Netherlands, April 2014.

[10] E. Damosso and L. M. Correia, Eds., *Digital mobile radio towards future generation systems*, final report ed. European Commission, 1999. [Online]. Available: http://www.lx.it.pt/cost231/final_report.htm

[11] W. C. Stone, "Electromagnetic signal attenuation in construction materials," NIST Building and Fire Research Laboratory, Gaithersburg, Maryland, NISTIR 6055 Report No. 3 6055, Oct. 1997.

[12] L. M. Frazier, "Radar surveillance through solid materials," in *Proceedings of the SPIE - The International Society for Optical Engineering*, vol. 2938, Hughes Missile Syst. Co., Rancho Cucamonga, CA, USA, 1997, pp. 139 – 146.

[13] R. Wilson, "Propagation losses through common building materials 2.4 GHz vs 5 GHz," University of Southern California, CA, Tech. Rep. E10589, Aug. 2002.

[14] C. A. Remley, G. H. Koepke, C. L. Holloway, C. A. Grosvenor, D. G. Camell, J. M. Ladbury, R. Johnk, D. R. Novotny, W. F. Young, G. Hough, M. McKinley, Y. Becquet, and J. Korsnes, "Measurements to support modulated-signal radio transmissions for the public-safety sector," NIST, Boulder, CO, Tech. Rep. Tech. Note 1546, Apr. 2008.

[15] F. Harrysson, J. Medbo, A. F. Molisch, A. J. Johansson, and F. Tufvesson, "Efficient experimental evaluation of a MIMO handset with user influence," *IEEE Trans. Wireless Commun.*, vol. 9, no. 2, pp. 853–863, Feb. 2010.

[16] J. Ø. Nielsen, B. Yanakiev, I. B. Bonev, M. Christensen, and G. F. Pedersen, "User influence on MIMO channel capacity for handsets in data mode operation," *IEEE Trans. Antennas Propagat.*, vol. 60, no. 2, pp. 633–643, Feb. 2012.